Available online at www.sciencedirect.com
SCIENCE DIRECT®
Journal of Nuclear Materials 320 (2003) 96–105
journal of nuclear materials
www.elsevier.com/locate/jnucmat

Study of a zirconia based inert matrix fuel under irradiation

C. Degueldre *, Ch. Hellwig

Laboratory for Materials Behaviour, Nuclear Energy and Safety, Paul Scherrer Institut, 5232 Villigen-PSI, Switzerland

Abstract

Yttria-stabilised zirconia doped with erbia and plutonia has been selected as inert matrix fuel (IMF) at PSI, Switzerland. The results of experimental irradiation experiments on yttria-stabilised zirconia doped with erbia and thoria samples utilising accelerators, tests with yttria-stabilised zirconia doped with plutonia and erbia or urania pellets within research reactors, and a study of natural zirconia contacted to actinide rich rock are evaluated and compared. The results obtained for zirconia implantation with xenon as a representative fission product are analysed in term of swelling and inertness of the material. The reactor tests preformed in the material test Boiling Water Reactor, Halden and in the High Flux Reactor, Petten are also described, with emphasis on the IMF properties under in-pile irradiation. The natural analogue study of baddeleyite from Jacupiranga, southern Brazil, provides additional information. Baddeleyite crystals enclosed within uranpyrochlore grains and received intense irradiation, which did not affect either the structural integrity or the durability of the mineral. The results of these case studies, with accelerator, use in-pile and contacted with natural radioactive sources, provide useful information on the outstanding of the behaviour of zirconia under irradiation.

1. Introduction

The research program on inert matrix fuels (IMFs) has led to the selection of yttria-stabilised zirconia (YSZ) doped with erbia and plutonia at PSI, Switzerland [1,2]. This IMF is foreseen to utilise plutonium in light water reactor (LWR) and to destroy it in a more effective way than possible with MOX. After utilisation in LWR, the plutonium isotopic vector in the spent IMF foreseen for direct disposal will be devaluated far beyond the standard spent fuel.

The physical properties of the material depend on the choice of stabiliser as well as on other dopants such as burnable poison and fissile material. Among them, the behaviour under irradiation is primordial for utilisation in-pile. This property has been studied utilising *accelerator* ion beams and observing material changes during irradiation or implantation with heavy ion e.g. [3]. Synthetic zirconia's in the stabilised cubic form behaves like other fluorite structure types (e.g., CeO_2, ThO_2 and UO_2) and is highly resistant to amorphization by neutrons [4] or fission tracks [5].

As a result of an iterative study, a $(Er,Y,Pu,Zr)O_{2-x}$ solid solution with defined fraction of fissile and burnable poison was selected as fuel material for tests in *research reactors*. Zirconia based IMF material has been fabricated for irradiation experiments in the material test Boiling Water Reactor, Halden [6] and in the High Flux Reactor, Petten [7]. For the material qualification, relevant fuel properties were considered. Among them, in-pile behaviour and stability are key properties for the fuel in reactor as well as for the geologic disposal of the spent fuel.

Baddeleyite, the natural ZrO_2 monoclinic mineral, is of potential interest as a *natural analogue* for spent zirconia based IMF designed for the safe geological disposal of this high level nuclear waste [1,8,9]. Natural analogues provide information for the assessment of the long-term performance of nuclear waste forms primarily in three areas: crystal chemistry, geochemical alteration, and radiation damage effects [10,11]. Studies in all three

* Corresponding author. Tel.: +41-56 3104176; fax: +41-56 3102203.
E-mail address: claude.degueldre@psi.ch (C. Degueldre).

0022-3115/03/$ - see front matter © 2003 Elsevier Science B.V. All rights reserved.
doi:10.1016/S0022-3115(03)00175-2

of these areas using natural baddeleyite may provide useful information concerning the long-term performance of non-stabilised monoclinic ZrO_2. The usefulness of natural analogue studies for the evaluation of materials such as IMF may be restricted due to differences in the composition and structure of baddeleyite and stabilised-ZrO_2; however, it is anticipated that at least some application may arise in the areas of crystal chemistry and especially radiation damage effects. Section 3.3 concerns the case study of baddeleyite from the Jacupiranga carbonatite complex of southern Brazil.

This study describes and compares the behaviour of zirconia under irradiation with accelerators, within research reactors and contacted with natural radioactive sources. This study aims to provide information on the behaviour of zirconia under irradiation.

2. Experimental

2.1. Zirconia samples

2.1.1. Samples for accelerator target

Additives such as Y_2O_3 or Ln_2O_3 (Ln for lanthanide) are currently used to stabilise zirconia. In addition to yttria and erbia, thorium dioxide was occasionally added to the zirconium dioxide matrix. The fabrication for the preparation of the material applied a wet route including co-precipitation of the oxy-hydroxide phase by gelation e.g. [12] starting with the nitrate solutions. The samples were dried, calcined, grinded, pelletized and sintered.

To prepare the inert matrix material for electron microscopy, disks of 3 mm in diameter were made with an ultrasonic cutter. These discs were dimpled into 10–20 μm in thickness at the centre part of the discs. Perforation was made by thinning with a 3 keV Ar^+ ion beam at an angle of 20° to the surface of the disks. Final polishing was carried out with 2 keV at 15°. All thinning was done at ambient temperature.

Simulated fuel with thorium instead of plutonium was also investigated. The thorium derived simulated fuel was prepared following a similar route. $Er_{0.05}Y_{0.10}Th_{0.10}Zr_{0.75}O_{1.925}$ samples were prepared to investigate the microscopic behaviour of the material under irradiation. TEM sub-samples were also prepared by mechanical grinding and ion milling. The thickness of such samples was of the order of 100 nm.

2.1.2. Reactor fuel fabrication

Fabrication of the $(Er,Y,Pu,Zr)O_{2-x}$ IMF can be carried out with the similar process steps as for current-day MOX fuel. Two fabrication routes, i.e. a dry route including attrition milling (ATT) and a wet route with co-precipitation (CO), were followed for the fuel material fabrication [13].

For IMF-ATT, the powder constituents (ZrO_2, PuO_2, Y_2O_3 and Er_2O_3) were mixed together mechanically in a vessel and milled to a homogeneous powder in an attrition mill. The powder was pressed to pellets and sintered at 1723 K in a CO_2 atmosphere to a pellet relative density of 95%. The grain size could not be determined exactly but was clearly below 5 μm.

For IMF-CO, microspheres with the desired composition were produced by internal gelation, dried and calcined in argon atmosphere. The calcined spheres were crushed to particles and milled in the attrition mill to fine powder. This powder was pressed to pellets and sintered at 1973 K in an N_2/H_2 atmosphere to a pellet relative density of 92% for one batch and 86% for a second. The grain size was in the order of 25 μm.

For the Halden test, three rodlets of IMF, two IMF-ATT and the third one IMF-CO, were fabricated. The three MOX segments used for comparison comprised two MOX rodlets prepared at PSI and the third was a reference MOX prepared at BNFL by the short-binderless route (MOX-SBR). For the test carried out at the High Flux Reactor, the samples were both $(Er,Y,Pu,Zr)O_{2-x}$ and $(Y,Pu,U,Zr)O_{2-x}$ solid solutions fabricated by co-precipitation by internal gelation from the nitrate solutions, crushing, milling of the dry microspheres, compaction and sintering at 2023 K in an N_2/H_2 atmosphere. The fissile Pu concentration of these materials was 0.41 $g\,cm^{-3}$.

2.1.3. Natural samples

The baddeleyite (natural monoclinic ZrO_2) from the Jacupiranga carbonatite complex of southern Brazil provides some additional information on the crystal durability, and radiation damage effects of the mineral. Baddeleyite crystals in these samples are associated with small (~1 mm) uranpyrochlore crystals recovered from carbonatite. The baddeleyite occurs as colorless, flat plates or blades either intergrown with uranpyrochlore or more rarely, as millimeter to submillimeter single crystals or twinned crystals with no associated uranpyrochlore. The baddeleyite crystal morphology can be quite variable, especially within the confines of the uranpyrochlore host, where curved grain boundaries and embayments are also common.

2.2. Irradiation systems

2.2.1. Irradiation with accelerators

The inert matrix material was irradiated using an analytical electron microscope with a low energy Xe injector at the Japanese Atomic Energy Research Institute. Observations and irradiation experiments were performed in an electron microscope JEM-2000FXII modified equipped with a thermal field-emission electron source and a 40 keV ion accelerator. The ion beam was incident to the surface of the specimen at an angle of

60°. The beam comprised 60 keV Xe ions to provide a Xe flux of 5×10^{12} cm^{-2} s^{-1}. The irradiations were carried out at room temperature and at 925 K with large Xe doses (2×10^{16} cm^{-2}), simulating the situation in light water reactor conditions. The penetration depth of the Xe ions in the inert matrix irradiated with 60 keV Xe ion was estimated to about 15 nm by the SRIM code [14] using a displacement energy $E_d = 60$ eV. All the irradiations were carried out for 1 h; the fluence of Xe ions was 1.8×10^{16} cm^{-2}.

A pre-thinned (Er,Y,Th,Zr)O_{2-x} TEM specimen was irradiated using the HVEM-Tandem Facility at Argonne National Laboratory (ANL). The material was irradiated with a Xe ion dose rate of 3.4×10^{12} cm^{-2} s^{-1}, to Xe doses of 2×10^{16} cm^{-2} with 1.5 MeV Xe ions.

2.2.2. Irradiation in reactor

The irradiation of the experiment IFA-651.1 with IMF based on yttria-stabilised zirconia (YSZ) and with MOX fuel started as a part of the OECD Halden Reactor Project at end of June 2000 [15]. The aim of this experiment is to measure the central line temperature change with burn-up, the fission gas release, the densification, the swelling and the general thermal behaviour of these fuels during irradiation. The rods are equipped with expansion thermometers (ETs): rods 3&5, thermocouples (TFs): rods 2, 4, 1&6, and/or stack elongation detectors (EFs) rods: 2, 4&6. All rods were equipped with pressure transducers (PFs). In order to get a good record of the axial power distribution, the assembly is instrumented with three axial neutron detectors (ND). The radial power profile will be determined by three NDs, which are placed in the axial centre of the assembly. The Halden reactor is a boiling heavy water cooled and moderated reactor with a thermal power of 18–20 MW. The moderator temperature is about 510 K and the reactor includes 35 instrumented fuel assemblies and 70 drivers assemblies. For the current ongoing tests, the burnup will reach 490 kW d cm^{-3}, or 540 MW d kg^{-1} of heavy metal (or 54 MW d kg^{-1} of heavy metal for MOX) in 1000 full power days corresponding to 57% of plutonium reduction.

The OTTO sample holder has been irradiated for at least 22 cycles (545 full power days) in the High Flux Reactor (HFR), Petten, in-core position H8 [6]. The obtained total neutron fluence will be approximately 1×10^{26} m^{-2} at the end of the irradiation. Six IMF samples were tested including capsules 1 and 2 loaded with zirconia solid solutions: (Er,Y,Pu,Zr)O_{2-x} and (Y,Pu,U,Zr)O_{2-x} respectively. They are compared with a MOX sample (7). The goal of the OTTO irradiation is to reach a high Pu burnup, and the anticipated (^{239}Pu + ^{241}Pu) burnup at the end of irradiation is about 70%. The diameter of the pellets is 8.00 mm. The pellets were encapsulated in Zircaloy-4 cladding tubes with an inner diameter of 8.22 mm and an outer diameter of 9.00 mm. The 2-D WIMS7 code package is used to calculate the fission power for each of the pins, each of which have a target length of 7 cm. This code package averages flux over the core height, which is 60 cm. The real power of each of the seven pins is calculated using a known flux profile for the core position and taking the axial positions of the pins and their corresponding flux buckling into account.

2.2.3. Irradiation with natural system

The irradiation of the baddeleyite from Jacupiranga, is mostly due to the actinides and filiations nuclides decays from the uranpyrochlore adjacent material. The alpha-decay dose and displacements per atom (dpa) are calculated for baddeleyite in the case study using the range of measured U and Th concentrations and the crystallisation age by using the following equations:

$$D = 6 \cdot N_{232\mathrm{Th}} \cdot (e^{\lambda_{232\mathrm{Th}} \cdot t} - 1) + 8 \cdot N_{238\mathrm{U}} \cdot (e^{\lambda_{238\mathrm{U}} \cdot t} - 1), \quad (1)$$

$$\mathrm{dpa} = \frac{1500 \cdot D \cdot M_f}{N_A \cdot N_f}. \quad (2)$$

In Eq. (1), $N_{232\mathrm{Th}}$ and $N_{238\mathrm{U}}$ represent the present numbers of atoms of ^{232}Th and ^{238}U, $\lambda_{232\mathrm{Th}}$ and $\lambda_{238\mathrm{U}}$ are their decay constants, and t is the geological age. Note that no consideration was given to the presence of ^{235}U ($7 \cdot N_{235\mathrm{U}} \cdot (e^{\lambda 235\mathrm{U} \cdot t} - 1)$), which accounts for a very small fraction of the total U concentration. In Eq. (2), M_f is the molecular weight of one formula unit, N_A is Avogadro constant, and N_f is the number of atoms per formula unit. The cumulative alpha-decay doses was calculated. The geological age, for the baddeleyite formation is of the order of 130 million years. This applies to both the internal irradiation and external irradiation from pyrochlore since baddeleyite and pyrochlore have essentially the same age.

3. Results

3.1. Ion irradiation and implantation using accelerators

The damage, retention and diffusion of cesium, xenon and iodine in inert matrix has been investigated by implanting ions in zirconia inert matrix material. These implantations up to the at% doses in the solid solution did not amorphize the material as already described earlier e.g. Degueldre et al. [16].

3.1.1. Xe ion irradiation at low energy

At room temperature small defect clusters of about 1 nm in diameter were formed at an early stage, at the

Xe fluence of 3×10^{14} cm^{-2}, at room temperature. Then small bubbles of about 0.3 nm in diameter were formed at Xe fluence of 1.5×10^{15} cm^{-2}. The density of bubbles increased up to the Xe fluence of about 3×10^{15} cm^{-2}. The bubble size grew with increasing fluence and their diameters were ranging from 0.5 to 2.5 nm at Xe fluence of 1.8×10^{16} cm^{-2}. The electron diffraction patterns show that no amorphization occurred.

At 925 K very small defect clusters with size <1 nm were formed at an early stage with Xe fluence of 1.5×10^{14} cm^{-2} as shown in Fig. 1(a). Then small bubbles of about 0.5 nm in diameter were formed at a Xe fluence of 6×10^{14} cm^{-2} as shown in Fig. 1(b). With increasing fluence, bubbles grew and collapsed with each other as shown in Fig. 1(c)–(d). Amorphization was not observed after irradiation at 925 K to Xe fluence of 1.8×10^{16} cm^{-2}, as can be seen in Fig. 1(d).

After ion irradiation, the volume swelling of the specimens was calculated from the total bubble volume estimated from their densities and average radius. The average bubble radius was about 0.46 nm at room temperature and about 1.44 nm at 925 K at a Xe fluence 1.8×10^{16} cm^{-2}. The volume swelling was estimated to be about 0.19% at room temperature and about 0.72% at 925 K, respectively. On the inert matrix with erbia, formation of bubbles at the surface was observed on-line above 10–15 displacements per atom (dpa) that may induce the swelling of the material.

3.1.2. Xe ion irradiation at high energy

TEM analysis has shown that the studied $Er_{0.05}Y_{0.10}Th_{0.10}Zr_{0.75}O_{1.925}$ polycrystalline sample had grain sizes varying from 500 nm to several micrometers. The material was irradiated with 1.5 MeV Xe ions at an ion dose rate of 3.4×10^{12} cm^{-2} s^{-1} using the HVEM-Tandem Facility at ANL. Irradiation was performed at 20 K with a liquid helium stage, because previous experiences on ZrO_2 have shown that the phase did not amorphize at low temperatures. Observations were carried out on-line. In the specimen irradiated at 20 K with large full Xe doses of 2×10^{16} cm^{-2}, the damage level of the material was observed off-line. No amorphization was observed by in-situ observation of the electron diffraction pattern. According to SRIM calculation, the damage in the 100 nm depth of the TEM foil reached 25 dpa at full ion dose.

The irradiation induced the formation of dislocation loops. At a Xe fluence of 2×10^{14} cm^{-2}, a low density of dislocation loops was reported. At a Xe fluence of 2×10^{16} cm^{-2}, a higher density of dislocation loops was observed with sizes ranging from 20 to 60 nm. It was very difficult to determine the interstitial/vacancy nature of the loops due to the high density. TEM analysis after ion irradiation did not reveal any amorphization even near the grain boundaries (Fig. 2(a)). In some grains, 3-D vacancy clusters (voids) of 20–60 nm were observed (Fig. 2(b)). The results of this study indicate that the irradiation temperature (20 K) is still too high to amorphize stabilised zirconia.

3.2. Investigations in pile

Two irradiation experiments started in 2000: the Halden Reactor experiment IFA-651.1 [7], which is devoted to yttrium stabilised zirconia doped with plutonium and the OTTO experiment in the HFR, Petten [6] which involved various types of Pu-IMF and ended late 2002.

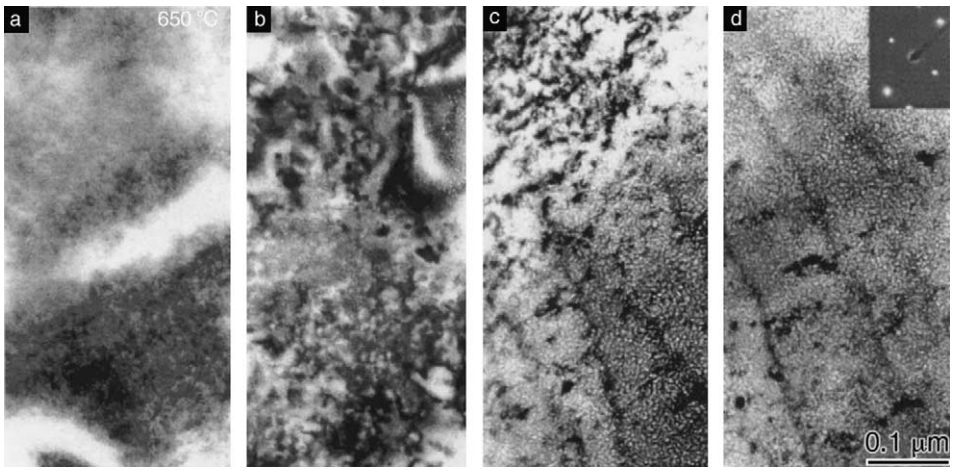

Fig. 1. Processes of formation and growth of defect clusters and bubble formation in $Er_{0.05}Y_{0.10}Zr_{0.85}O_{1.925}$ during irradiation with Xe ions. Conditions: 60 keV Xe ions with dose rate of 5×10^{12} cm^{-2} s^{-1} at 925 K. Xe fluence: (a) 1.5×10^{14} cm^{-2} (defect clusters were formed), (b) 6×10^{14} cm^{-2} (bubbles were formed), (c) 6×10^{15} cm^{-2}, (d) 1.8×10^{16} cm^{-2} the material is still crystalline. Data from Ref. [21].

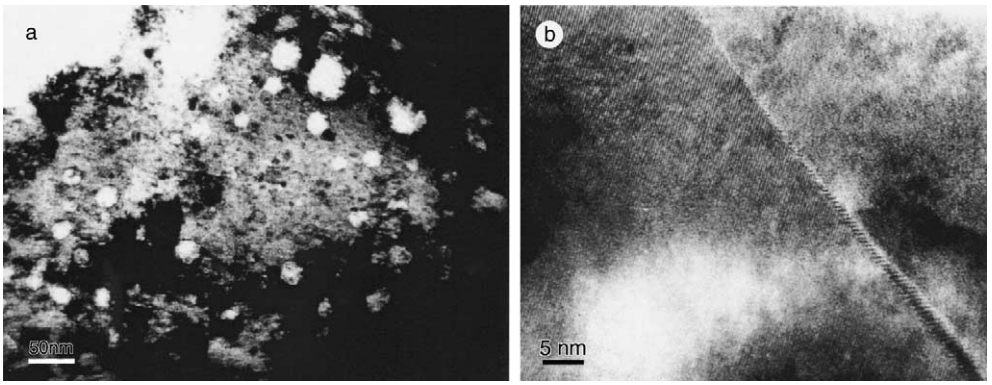

Fig. 2. TEM bright-field images of a 1.5 MeV Xe ion irradiated sample (20 K). Conditions: material $Er_{0.05}Y_{0.10}Th_{0.10}Zr_{0.75}O_{1.925}$, (a) HRTEM image showing the sample is still crystalline even near the grain boundaries (Xe fluence 2×10^{16} cm^{-2}), (b) image showing the formation of small voids (Xe fluence 2×10^{16} cm^{-2}). Data from Ref. [21].

3.2.1. Results from the IMF testing in the Halden Reactor

Three IMF and three MOX specially fabricated rodlets are being used for the in-pile testing in the Instrumented Fuel Assembly IFA-651.1. The irradiation experiment, conducted in the framework of the OECD Halden Reactor Project, started towards the end of June 2000, and is scheduled to last till 2005.

The principal aim of the experiment is to measure the central-line temperature, its change with burnup, fission gas release, densification, swelling and the general thermal behaviour of the fuels. The first cycle was completed after 120 days, and a 47 kW d cm^{-3} (i.e. 4.5 MW d kg^{-1} of MOX) average assembly burnup was attained. Note that this unconventional unit for burnup (energy released per unit volume) was chosen in order to be able to compare IMF and MOX fuel with their very different densities.

Fig. 3 shows the measured fuel centre-line temperatures during the course of the first cycle. After 15.5 days the maximum power of the IMF and MOX rodlets (~25 kW m^{-1} average) was achieved. The irradiation cycle lasted some 120 days in total. The measured temperatures are within the expected range for both IMF and MOX, the higher temperatures in the former rodlets reflecting the significantly lower thermal conductivity of IMF.

The IMF densification is unexpectedly high as indicated by the rod inner pressure measurements. The IMF-ATT rods sinter to nearly 100% theoretical density within 35 kW d cm^{-3} burnup. IMF-CO shows a slower densification, which might be explained by its larger grain size and the variations in the fabrication process (sintering in a oxidative versus reductive atmosphere). In spite of the strong densification, the IMF temperature has remained relatively stable (see Fig. 3). This might be explained by the formation of a central void region while the outer pellet diameter (and hence the gap size) stays nearly unaffected. However, only post irradiation examinations will reveal the effective process.

3.2.2. Results from IMF testing in High Flux Reactor, Petten

The neutron radiography of all the seven pins of the OTTO experiments were taken before irradiation, after 0.10 cycles (2.5 full power days), after 1.05 cycles (26.5 full power days), after seven cycles of irradiation (175 full power days), and after 14 cycles (350 full power days). Fig. 4 shows an example of neutron radiography of both pins 1 and 2. These radiographies allow measurement of the length and diameter of the IMF pellet segments and detailed investigations of the pellet morphology. The zirconia solid solutions segments present no large size variation. The length change after cycle 1.05 (25 full power days) were -1.30 ± 0.07 and $1.03 \pm 0.07\%$ for $(Er,Y,Pu,Zr)O_{2-x}$ and $(Y,Pu,U,Zr)O_{2-x}$ respectively. These changes are comparable with those observed for the MOX reference material which variation is $1.25 \pm 0.07\%$ for the same irradiation period. The retraction of the IMF segment during this first irradiation period may be due to a reorganisation of the material, which may explain the pressure decrease during the first cycle of the Halden experiment.

3.3. Natural analogue

The baddeleyite crystals in the samples recovered from the carbonatite are associated with small (~1 mm) uranpyrochlore crystals. An example of the intergrowths with uranpyrochlore is shown in Fig. 5. The images reveal that the baddeleyite crystal morphology can be quite variable, especially within the confines of the uranpyrochlore host.

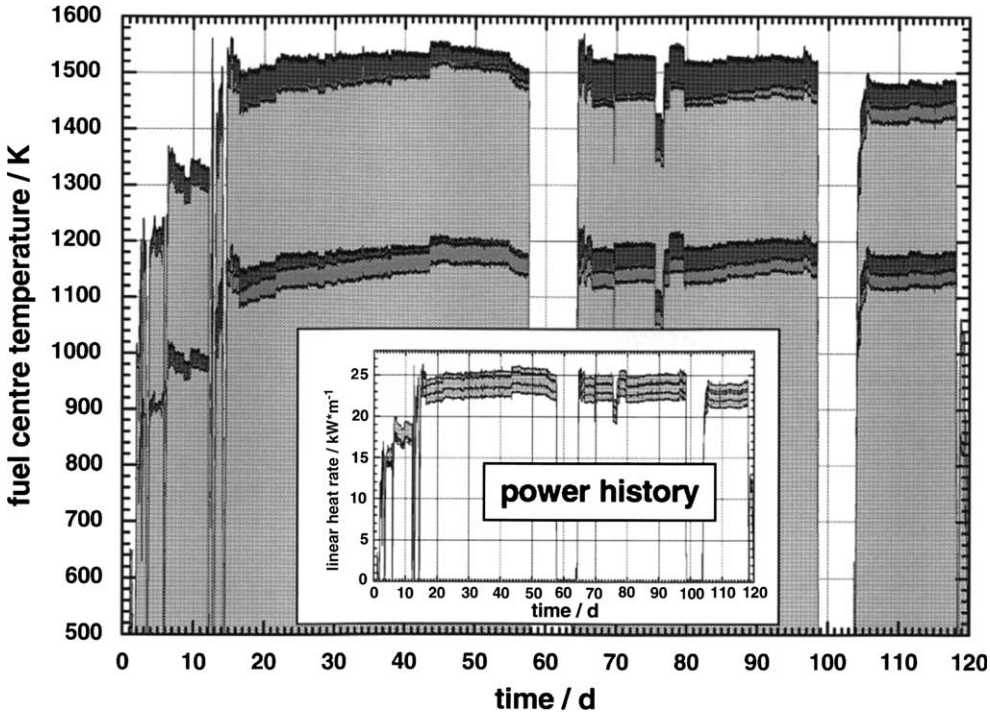

Fig. 3. Central temperature of the three IMF and of the three MOX segments during the first cycle of the irradiation of the experiment IFA-651.1 in the Halden Boiling Water Reactor. Data from Ref. [22] with from highest to lowest temperature: IMF-ATT (rod 5), IMF-ATT (rod 2), IMF-CO (rod 4), MOX-ATT (rod 3), MOX-SBR (rod 1) and MOX-ATT (rod 6).

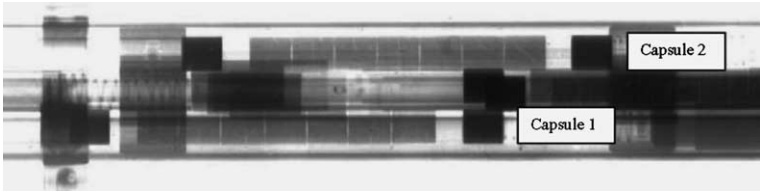

Fig. 4. Neutron radiography of the pins 1 and 2 in sample holder after cycle 01.05. Conditions: the top of the pins are positioned at the right side, irradiation 26.5 full power days in the High Flux Reactor, Petten. Data with courtesy from Ref. [23].

3.3.1. Morphological observations

Further studies of the uranpyrochlore have been carried out in order to document the alteration environment of the associated baddeleyite. The SEM images revealed that the uranpyrochlore host phase contains irregular, microfractured zones of alteration. SEM–EDX analyses of unaltered and altered areas generally show that the alteration involved removal of Na by the fluid phase, accompanied in some areas by minor depletion in Ca. A significant feature of the uranpyrochlore is that the Th and U concentrations remain unaffected by the alteration, confirming earlier work [17]. In every intergrowth examined, the associated baddeleyite crystals do not appear to have been affected by the alteration (Fig. 5(c) and (d)). SEM images of the uranpyrochlore and baddeleyite show that the baddeleyite is relatively unfractured and has uniform contrast. There is no evidence for alteration along any of the existing fractures in the baddeleyite, even though the aqueous fluid phase clearly had access to these areas. The baddeleyite immediately adjacent to the grain boundary is also unaltered, despite being subjected to irradiation by alpha-recoil nuclei and alpha-particles emitted by the associated uranpyrochlore.

3.3.2. Radiation damage effects

Total actinides are generally below 2000 ppm, but can result in an internal cumulative alpha-decay doses of up to 1×10^{16} mg^{-1} for samples with ages of up to 2×10^{9} years.

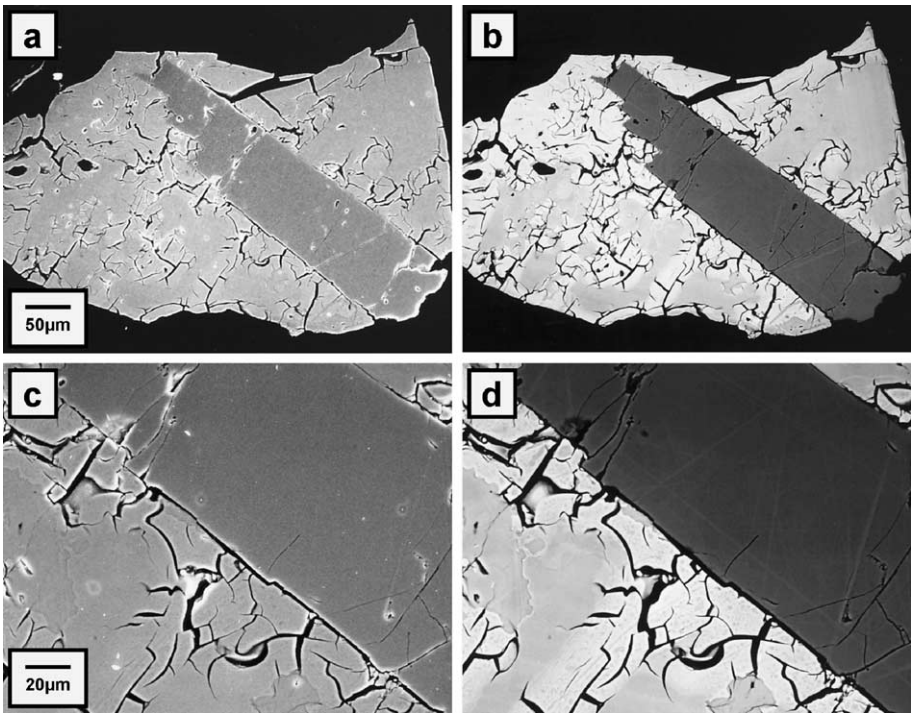

Fig. 5. Secondary electron (a,c) and backscattered electron image (b,d) pairs of intergrowth between uranpyrochlore and baddeleyite. Images taken at low magnifcation (a,b) illustrate microfracturing morphology of the uranpyrochlore (lighter gray) and the more regular morphology of the baddeleyite (darker gray). Higher magnification images (c,d) show details of microfracturing and alteration. Data from Ref. [24].

Eqs. (1) and (2), and the measured U concentrations of baddeleyite were used to calculate an alpha dose range of $0.02–0.09 \times 10^{16}$ mg^{-1}, equivalent to 0.02–0.09 dpa based on the assumption that there are 1500 displacements per alpha-decay event. This assumption was investigated further using the software package TRIM [14]. Unfortunately, there are no reliable measurements of the displacement energies of Zr and O in baddeleyite or any other zirconium oxide or silicate phase. Recently Weber et al. [18] indicated E_d ranges from 20 to 55 eV for metal cations and from 20 to 70 eV for oxygen in several simple oxide structures. The average displacement energies of these compounds range around 25–45 eV; therefore, based on the SRIM simulations the calculated dpa values reported above may be overestimated by about a factor of approximately 1.5–2.5.

TEM results demonstrated [24] that the internal alpha-decay damage has had very little effect on the crystallinity and microstructure of the natural baddeleyite. The TEM images showed that none of the microstructural features typical of the crystalline–amorphous transformation documented previously for a number of oxide and silicate phases [19,20]. The zone axis electron diffraction patterns are sharp and there is no evidence for the presence of a diffuse ring, even when the crystal is tilted away from the zone axis diffraction condition. The cumulative dose of the baddeleyite core region is near the beginning of the crystalline–amorphous transformation in other minerals (e.g., pyrochlore, zirconolite, zircon), suggesting that baddeleyite may be more resistant to alpha-decay damage, but it is difficult to make any further assessment of the data, especially since the dpa values may be an overestimate.

A secondary source of damage exists for the baddeleyite grains intergrown with uranpyrochlore. In this case, the baddeleyite will have received an additional alpha-decay dose from the adjacent uranpyrochlore crystals. The additional dose received by the baddeleyite decreases from 50% of the dose of the uranpyrochlore at the grain boundary down to zero just beyond the maximum depth of penetration for recoil atoms and alpha-particles. SRIM simulations indicate that the recoil atoms will penetrate to approximately 19 nm and that the alpha-particles will penetrate to just over 10 μm on average. The associated uranpyrochlore crystals generally contain 19–26 wt% UO_2 and 0.3–3.5 wt% ThO_2, from which an alpha dose range of $6–9 \times 10^{16}$ mg^{-1} is calculated. Therefore, the alpha-decay dose of the adjacent baddeleyite ranges from 3 to 4.5×10^{16} mg^{-1} at the grain boundary down to the internal dose ($0.02–0.09 \times 10^{16}$

mg^{-1}). Regions of baddeleyite close to the grain boundary were also investigated by TEM. Bright field images and diffraction patterns indicated that these areas have developed a modified microstructure characterised by heavily strained and rotated crystalline domains. Measurements using dark field images indicated that the domain size is on the order of 5–20 nm and that the fine scale modulation is approximately 1 nm. There is little evidence for the formation of amorphous domains in these areas of baddeleyite near the grain boundary, as shown by the lack of diffuse rings in the diffraction pattern.

4. Discussion and concluding remarks

The zirconia inert matrix is a very robust stable material that forms solid solutions with numerous

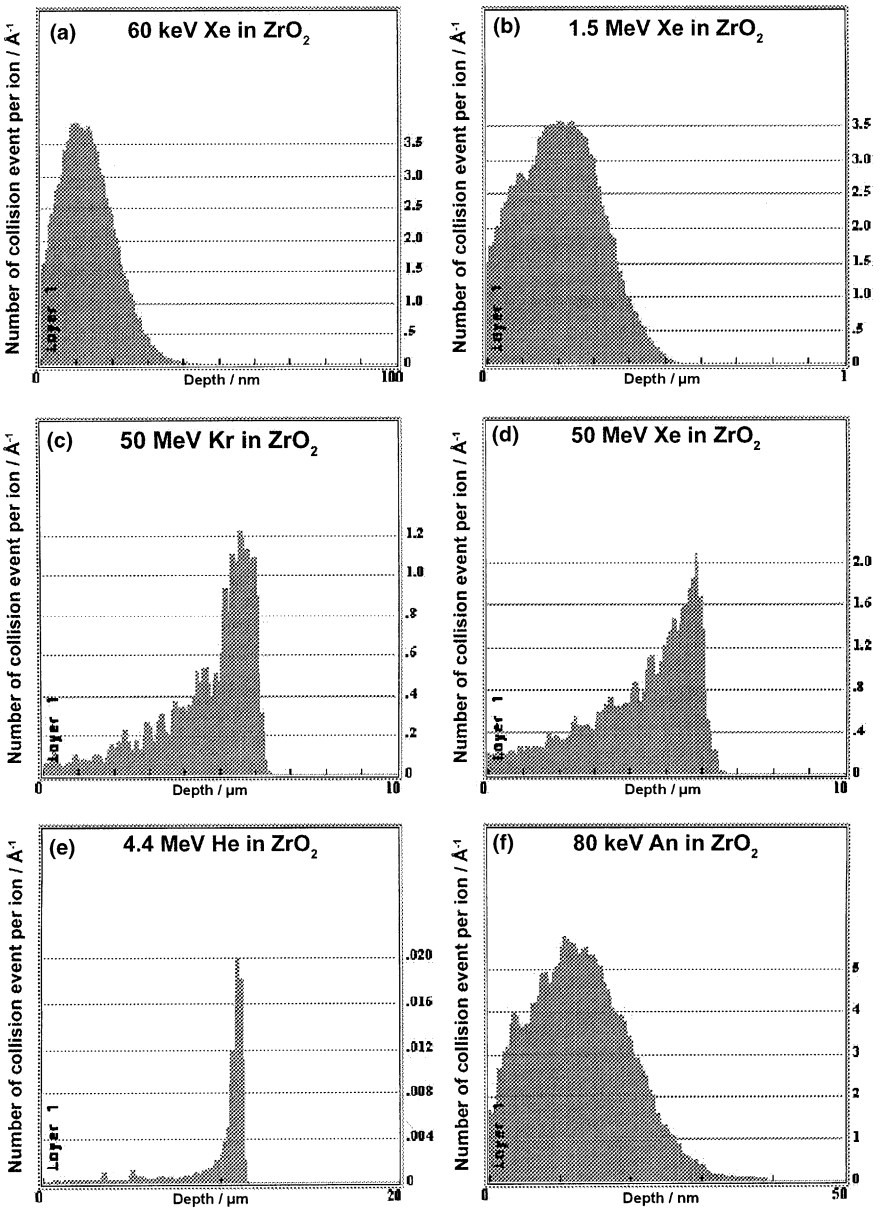

Fig. 6. Comparison of damages evaluated by TRIM in zirconia ZrO_2 for the three studied cases. In *Accelerator* target with 60 keV (a) and 1.5 MeV Xe (b); in *reactor* fuel with 50 MeV Kr (c) and 50 MeV Xe (d); in the *natural* sample with 4.5 MeV He (e) and 80 keV Th (f).

Table 1
Comparison of the parameters and results of the three case studies reported in this work. In these case studies no zirconia amorphization is observed or deduced

Irradiation system	Material	Particle	Energy (MeV)	Damage (dpa)	Dosis[a] (g^{-1})	Time (s)	Temperature (K)
Accelerator	(Er,Y,Th,Zr)O_2	Xe	0.06–1.50	15–25	$\sim 3 \times 10^{20}$	5×10^{-4}	273–950
Reactor	(Er,Y,Pu,Zr)O_2	(n), FP	20–200	10–50	$\sim 2 \times 10^{19}$[b]	1–5	500–2000
Natural source	ZrO_2	α, recoil	0–5	0–2.5	$\sim 10^{20}$	1.3×10^{8}	700

[a] Ion, FP, α or recoil ion dosis.
[b] For 10% Pu burnt in IMF.

elements such as lanthanides, transition elements or fission products. These inert material samples were produced with a theoretical density more than 90% using the co-precipitation method (wet fabrication procedure) or ATT (dry route) followed by pelletizing and sintering. These zirconia samples were tested for their behaviour under irradiation using accelerator or research reactors. Results are compared with those gained for a natural zirconia samples that have been contacted with an actinide rich mineral over geological times. Comparison of the damage created during ion bombardment and evaluated by TRIM is shown in Fig. 6. Comparison of damages in zirconia for the three studied cases i.e. in *accelerator* target (a–b), in *reactor* fuel (c–d) and in the *natural* analogue case (e–f).

4.1. Results from irradiation with accelerators

No amorphization was observed under Xe irradiation even under extreme conditions, including for example low energy Xe and bubble formation, or high energy Xe and low temperature (20 K). Swelling rates were estimated to be 0.19% at room temperature and 0.72% at 925 K during irradiation of the zirconia inert matrix with low energy Xe ions up to a Xe fluence of 1.8×10^{16} cm^{-2}. This confirms the robustness of this inert matrix material even after 3–4 collisions per ion and Å (see Fig. 6(a)–(b)).

4.2. Results with samples in research reactors

The Halden Reactor and the High Flux Reactor experiments are complementary. At Halden, the measured fuel centre temperatures are within the expected range for both zirconia-IMF and MOX, the higher temperatures in the former rodlets reflecting the significantly lower thermal conductivity of IMF. The IMF densification is rather high as indicated by the rod inner pressure measurements after the first cycle (120 days). In spite of the strong densification, the IMF temperature is seen to remain relatively stable.

In the High Flux Reactor experiments, the zirconia solid solutions segments do not present large size variations during irradiation. The length changes observed e.g. for (Er,Y,Pu,Zr)O_{2-x} are comparable with those observed for the MOX reference material (~1%) after the first cycle (26 days). The slight retraction of the IMF segment during this first irradiation period may be due to a reorganisation of the material, which explains the pressure decrease during the first cycle of the Halden experiment. However, only post-irradiation examinations will reveal the effective processes. As seen on the neutron radiographies the material is apparently very stable, even after ~2 collisions per ion and Å (see Fig. 6(c)–(d)).

4.3. Results from the natural analogue

The limited evidence from the literature suggests that baddeleyite may be resistant to the effects of alpha-decay damage from ^{232}Th and ^{238}U atoms incorporated in dilute solid solution. This evidence is consistent with previous ion irradiation studies and is also supported to a certain extent by the case study presented above. However, the TEM results described in this natural analogue study document very restricted modifications of the microstructure of baddeleyite under intense alpha-particle irradiation by an adjacent actinide-rich phase. In this example, the bombardment by alpha particles apparently caused no structure changes as expected after ~0.02 collisions per He-ion and Å, see Fig. 6(e), and fine scale modulations with the recoil nuclides, with no significant degradation of the material crystallinity, even after ~5 collisions per ion and Å, see Fig. 6(f).

The results of the three case studies are summarized in Table 1. All results converge to the conclusion that under extreme irradiation conditions with extensive ion doses, zirconia remains crystalline and does not undergo amorphization under the current thermodynamic conditions.

Some questions are, however, still open in this new research field on zirconia IMF, e.g. the fuel behaviour under power transients, the change in thermal conductivity with irradiation, the fission gas retention potential, the leaching behaviour of spent fuel and the possibilities to enhance the thermal conductivity and/or plutonium loading and burning efficiency by modification of the additives.

References

[1] C. Degueldre, U. Kasemeyer, F. Botta, G. Ledergerber, in: W.M. Murphy, D.A. Knecht (Eds.), Scientific Basis for Nuclear Waste Management XIX, Mater. Res. Symp. Proc. 412 (1996) 15.

[2] C. Degueldre, J.M. Paratte, Nucl. Technol. 123 (1998) 21.

[3] K.E. Sickafus, Hj. Matzke, Th. Hartmann, K. Yasuda, J.A. Valdez, P. Chodak III, M. Nastasi, R.A. Verrall, J. Nucl. Mater. 274 (1999) 66.

[4] F.W. Clinard Jr., D.L. Rohr, W. Ranken, J. Am. Ceram. Soc. 60 (1977) 287.

[5] E.R. Vance, J.N. Boland, Radiat. Eff. 37 (1978) 237.

[6] U. Kasemeyer, C. Hellwig, Y.W. Lee, D.S. Song, G.A. Gates, W. Wiesenack, Proc. 6th IMF, Prog. Nucl. Energy 38 (2001) 309.

[7] R.P. Schram, K. Bakker, H. Hein, J.G. Boshoven, R. van der Laan, C. Sciolla, T. Yamashita, C. Hellwig, F. Ingold, R. Conrad, S. Casalta, Proc. 6th IMF, Progr. Nucl. Energy 38 (2001) 259.

[8] R.L. Garwin, in: W.M. Murphy, D.A. Knecht (Eds.), Scientific Basis for Nuclear Waste Management XIX, Mater. Res. Symp. Proc. 412 (1996) 3.

[9] T. Muromura, Y. Hinatsu, J. Nucl. Mater. 151 (1987) 55.

[10] G.R. Lumpkin, K.P. Hart, P.J. McGlinn, T.E. Payne, R. Gieré, C.T. Williams, Radiochim. Acta 66&67 (1994) 469.

[11] G.R. Lumpkin, R.C. Ewing, Am. Miner. 81 (1996) 1237.

[12] G. Ledergerber, C. Degueldre, P. Heimgartner, M.A. Pouchon, U. Kasemeyer, Proc. 6th IMF Workshop, Strasbourg, May 30–June 2 2000, Prog. Nucl. Energy, 38 (2001) 301.

[13] Y.W. Lee, H.S. Kim, S.H. Kim, C.Y. Joung, S.H. Na, G. Ledergerber, P. Heimgartner, M. Pouchon, M. Burghartz, J. Nucl. Mater. 274 (1999) 7.

[14] J.F. Ziegler, J.P. Biersack, U. Littmark, The Stopping and Range of Ions in Solids, Pergamon, New York, 1985. Available from <www.srim.org>.

[15] U. Kasemeyer, H.-K. Joo, G. Ledergerber, J. Nucl. Mater. 274 (1999) 160.

[16] C. Degueldre, M. Pouchon, M. Döbeli, K. Sickafus, K. Hojou, G. Ledergerber, S. Abolhassani-Dadras, Proc. 102nd Am. Ceram. Soc., J. Nucl. Mater. 289 (2001) 115.

[17] G.R. Lumpkin, R.C. Ewing, Am. Miner. 80 (1995) 732.

[18] W.J. Weber, R.C. Ewing, C.R.A. Catlow, T. Diaz de la Rubia, L.W. Hobbs, C. Kinoshita, Hj. Matzke, A.T. Motta, M. Nastasi, E.K.H. Salje, E.R. Vance, S.J. Zinkle, J. Mater. Res. (1998) 1434.

[19] G.R. Lumpkin, R.C. Ewing, Phys. Chem. Miner. 16 (1988) 2.

[20] T. Murakami, B.C. Chakoumakos, R.C. Ewing, G.R. Lumpkin, W.J. Weber, Am. Miner. 76 (1991) 1510.

[21] C. Degueldre, P. Heimgartner, G. Ledergerber, N. Sasajima, K. Hojou, T. Muromura, L. Wang, Mater. Res. Symp. Proc. 439 (1997) 625.

[22] Ch. Hellwig, U. Kasemeyer, G. Ledergerber, B.-H. Lee, Y.-W. Lee, R. Chawla, Ann. Nucl. Energy 30 (2003) 287.

[23] V. Smit-Groen, OTTO image analysis, NRG Internal Report, October 2001.

[24] G. Lumpkin, J. Nucl. Mater. 274 (1999) 206.